



# Effect of steel and synthetic fibers on flexural behavior of high-strength concrete beams reinforced with FRP bars

Jun-Mo Yang, Kyung-Hwan Min, Hyun-Oh Shin, Young-Soo Yoon \*

School of Civil, Environmental & Architectural Engineering, Korea University, Anam-dong 5-ga, Seongbuk-gu, Seoul 136-701, Republic of Korea

## ARTICLE INFO

### Article history:

Received 24 June 2011

Accepted 2 January 2012

Available online 10 January 2012

### Keywords:

A. Fiber

B. Strength

Fiber-reinforced polymer (FRP) bar

## ABSTRACT

Six high-strength concrete beam specimens reinforced with fiber-reinforced polymer (FRP) bars were constructed and tested. Three of the beams were reinforced with carbon FRP (CFRP) bars and the other three beams were reinforced with glass FRP (GFRP) bars as flexural reinforcements. Steel fibers and polyolefin synthetic fibers were used as reinforcing discrete fibers. An investigation was performed on the influence of the addition of fibers on load-carrying capacity, cracking response, and ductility. In addition, the test results were compared with the predictions for the ultimate flexural moment. The addition of fibers increased the first-cracking load, ultimate flexural strength, and ductility, and also mitigated the large crack width of the FRP bar-reinforced concrete beams.

© 2012 Elsevier Ltd. All rights reserved.

## 1. Introduction

Recently, there has been a rapid increase in the use of fiber-reinforced polymer (FRP) bars substituting for conventional steel bars for concrete structures. Because FRP materials are nonmagnetic and noncorrosive, the problem of electromagnetic interference and steel corrosion can be avoided with FRP bars. In addition, FRP bars have the advantages of high strength and light weight, and a number of design guides and national standards have been published to provide recommendations for the analysis, design, and construction of concrete structures reinforced with FRP bars [1–3]. However, due to the substantial differences in the physical and mechanical properties between FRP and conventional steel, the use of FRP bars is still a formidable challenge for engineers.

The elastic modulus of FRP bars is much less than that of steel bars. Glass fiber-reinforced polymer (GFRP) bars and aramid fiber-reinforced polymer (AFRP) bars have an elastic modulus of between 35 and 50 GPa, and the elastic modulus of carbon fiber-reinforced polymer (CFRP) bars is between 120 and 150 GPa. This low elastic modulus leads to higher deflection and larger crack width in FRP bar-reinforced concrete beams that have an equivalent reinforcement ratio to steel-reinforced concrete beams; therefore, both deflection and crack width must be checked for the serviceability limit state. In addition, while steel bars behave inelastically after yield strength, FRP bars show perfect elastic behavior up to failure. Since FRP bars are linear elastic to failure and fail in a brittle manner, a ductile steel-like failure does not oc-

cur in FRP bar-reinforced concrete beams. To avoid brittle failure, failure by concrete crushing (over-reinforced beams), which is generally avoided in steel-reinforced concrete design, is preferred in FRP bar-reinforced concrete design [1–4]. However, because concrete itself is a brittle material and high-strength concrete is even more brittle, the ductility of FRP bar-reinforced high-strength concrete beams is less than that of steel-reinforced concrete beams.

In order to overcome the problems in terms of deformability and ductility of concrete beams reinforced with FRP bars, an alternative solution using fiber reinforced concrete (FRC) was proposed. It is now well established that the addition of steel fibers improves the mechanical properties of concrete members. Steel fibers offer increased toughness, durability, and impact resistance, and control the initiation and growth of cracks [5]. Many researchers have proven that the addition of steel fibers increases the ductility of over-reinforced steel reinforced beams and high-strength steel reinforced beams [6,7]. However, few studies have been carried out on the effects of fibers on the behavior of concrete beams reinforced with FRP bars. It is likely that the efficiency of fibers for the FRP bar-reinforced beams, which have a large crack width and deep crack propagation, can be higher than that for steel-reinforced beams. In particular, because the failure of over-reinforced beams with FRP bars is controlled mainly by the concrete compressive strain, the increased and softened postpeak strain of FRC may considerably improve the ductility of FRP beams.

In this study, six high-strength concrete beam specimens were constructed and tested to investigate the effect of fibers on the behavior of FRP bar-reinforced concrete beams. Carbon FRP (CFRP) bars and glass FRP (GFRP) bars were used as flexural reinforcements, and not only steel fibers but also recently developed polyolefin synthetic fibers [8] were considered as reinforcing discrete

\* Corresponding author. Tel.: +82 2 3290 3320; fax: +82 2 928 7656.

E-mail addresses: [jmyang@korea.ac.kr](mailto:jmyang@korea.ac.kr) (J.-M. Yang), [ysyoon@korea.ac.kr](mailto:ysyoon@korea.ac.kr) (Y.-S. Yoon).

## Nomenclature

$A'_s$	area of compressive steel reinforcement, mm <sup>2</sup>	$h$	overall height of beam, mm
$A_r$	area of flexural reinforcements, mm <sup>2</sup>	$l_f$	fiber length, mm
$A_{r1}, A_{r2}$	area of outer layer and inner layer flexural reinforcements, respectively, mm <sup>2</sup>	$M_u$	ultimate moment, kN m
$b$	width of beam section, mm	$P_{cr}$	first cracking load, kN
$c$	distance from extreme compression fiber to the neutral axis, mm	$P_u$	ultimate load, kN
$C_c, C'_s$	compressive force of concrete and compressive steel reinforcement, respectively, kN	$S$	average slope of the load deflection curve
$d_f$	fiber diameter, mm	$T_{150}^D$	toughness of FRC, area under the load vs. net deflection curve 0 to $L/150$ , Nm
$d_1, d_2$	effective depth of outer layer and inner layer flexural reinforcements, respectively, mm	$T_f$	tensile force of fibrous concrete, kN
$D'$	depth of compressive steel reinforcement, mm	$T_{r1}, T_{r2}$	tensile force of outer layer and inner layer flexural reinforcements, respectively, kN
$D_f$	bond factor of steel fiber	$v_f$	percentage by volume of fibers, %
$e$	distance from extreme compression fiber to top of tensile stress block of fibrous concrete, mm	$V_f$	fiber volume content
$E_{ct}$	elastic modulus of concrete in tension, GPa	$w_f$	percentage by weight of fibers, %
$E_{el}$	elastic energy released upon failure, kN m	$\beta$	bond factor of fiber
$E_r$	modulus of elasticity of reinforcement, GPa	$\beta_1$	factor relating the depth of equivalent rectangular compressive stress block to the neutral axis depth
$E_{tot}$	total energy stored in the system, kN m	$\gamma$	multiplier on $f'_c$ to determine the intensity of an equivalent rectangular stress distribution for concrete
$f_c$	compressive stress of concrete, MPa	$\Delta_{cr}$	deflection at first cracking load, mm
$f'_c$	specified compressive strength of concrete, MPa	$\Delta_u$	deflection at ultimate load, mm
$f_{150}^D, f_{600}^D$	residual strength of FRC at net deflection of $L/150$ and $L/600$ , respectively, MPa	$\epsilon_c$	compressive strain in concrete
$f_r$	modulus of rupture of concrete, MPa	$\epsilon'_c$	strain corresponding to the peak stress of FRC
$f_{r1}, f_{r2}$	stress in outer layer and inner layer flexural reinforcements, respectively, MPa	$\epsilon_{cu}$	ultimate compressive strain in concrete
$f'_s$	stress in compressive steel reinforcement, MPa	$\epsilon_{r1}, \epsilon_{r2}$	strain in outer layer and inner layer flexural reinforcements, respectively
$f_{sp}$	splitting tensile strength of concrete, MPa	$\epsilon'_s$	strain in compressive steel reinforcement
$f_t$	maximum tensile strength of concrete, MPa	$\epsilon_f$	tensile strain in fibers at theoretical moment strength of beam
$f_u$	ultimate tensile strength of reinforcement, MPa	$\mu_e$	ductility index
$f_y$	specified yield strength of reinforcement, MPa	$\sigma_t$	tensile stress in fibrous concrete, MPa
$F_{be}$	bond efficiency of the fiber which varies from 1.0 to 1.2 depending upon fiber characteristics	$\tau$	interfacial bond stress between fiber and matrix, MPa

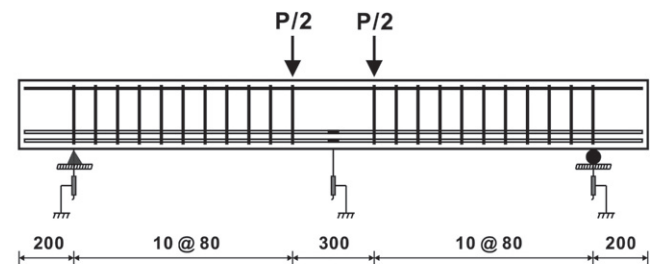
fibers. This is because the large crack width and deep crack propagation in FRP bar-reinforced concrete beams have a high potential for the corrosion of steel fibers at cracks, even if crack widths of less than 0.1 mm do not allow the corrosion of steel fibers passing across the crack [9]. This study focused on the flexural behavior of these beams in terms of load-carrying capacity, cracking pattern, and ductility. In addition, the experimental results presented in this paper were compared with the results from flexural strength prediction models proposed by various researchers [10–12].

## 2. Experimental program

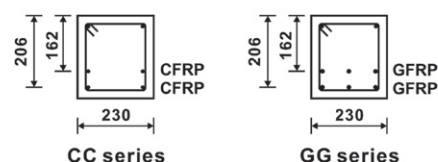
### 2.1. Test specimens

Fig. 1 and Table 1 show the details of six beam specimens. All specimens were 2300 mm long with a rectangular cross section of  $230 \times 250$  mm. These were reinforced with two layers of reinforcement, and the effective depths of the outer layer ( $d_1$ ) and the inner layer ( $d_2$ ) were 206 mm and 162 mm, respectively. The main variables were the material of the flexural reinforcement and the fiber. The specimens can be divided into two series: a beam series reinforced with CFRP bars (CC Series) and a beam series reinforced with GFRP bars (GG Series). In order to provide similar nominal flexural strength for the two series, four 9 mm CFRP bars were used in the CC Series beams, and six 13 mm GFRP bars were used in the GG Series beams. Each specimen was made of different types of concrete, i.e. plain concrete, steel fiber reinforced concrete (SFRC), and synthetic fiber reinforced concrete (SNFRC). The letters ST and

SN in the specimen names indicate steel fiber and synthetic fiber, respectively. The steel fibers and synthetic fibers were added to the SFRC in the percentage of  $v_f = 1.0\%$  by volume and to the SNFRC in the percentage of  $v_f = 2.0\%$  by volume. A 25 mm concrete cover



(a) Reinforcement details and the locations of strain gages and LVDTs



(b) Section details

Fig. 1. Details of test specimens and test setup (dimensions in mm).

Download English Version:

<https://daneshyari.com/en/article/818611>

Download Persian Version:

<https://daneshyari.com/article/818611>

[Daneshyari.com](https://daneshyari.com)